

Parallel plate analyser with second order focusing property

W Schmitz and W Mehlhorn†

Institute of Nuclear Physics, University of Münster, Germany

MS received 12 May 1971

Abstract The optical properties are studied of three different parallel plate analysers using point sources, the usual $\pi/4$ analyser with first order focusing and two versions of the $\pi/6$ analyser with second order focusing. It is shown that the ratio of the transmission to the resolution of a modified $\pi/6$ analyser, constructed in a 2π geometry, is superior to all other electrostatic analysers having a 2π geometry. Because parallel plate analysers with 2π geometry have the disadvantage of large ring detectors, sector shaped analysers with $\Delta\phi \ll 2\pi$, requiring only commercially available particle detectors, have also been investigated. The modified $\pi/6$ analyser is also superior to the other parallel plate analysers.

1 Introduction

In the low energy region (0–1000 eV) electrostatic energy analysers have certain advantages over magnetic analysers and have therefore been used extensively during recent years. Here the cylindrical mirror analyser (Gremmelmaier 1952, Blauth 1957, Mehlhorn 1960) and the parallel plate analyser (Harrower 1955) are distinguished by the fact that for point sources the focusing is of second order (Zashkvara *et al.* 1966, Sar-El 1967, Aksela *et al.* 1970, Green and Proca 1970, Proca and Green 1970) whereas for the other electrostatic analysers (127° cylindrical analyser (Hughes and Rojansky 1929) and spherical plate analyser (Purcell 1938)) focusing is only of first order. Furthermore, the cylindrical mirror analyser – like the spherical plate analyser – has the additional advantage of two dimensional focusing in devices using axially symmetric beams.

Hafner *et al.* (1968) have shown recently that for point sources the ratio of transmission to resolution for the cylindrical mirror analyser is superior to that for the spherical analyser, provided the exit slit of the mirror analyser coincides with the minimum trace width, which does not occur at the position of second order focusing.

In spite of the fact that the parallel plate analyser with first order focusing (Harrower 1955) is inferior to the two last mentioned analysers, it has often been used (Lassettre *et al.* 1964, Edelmann and Ulmer 1965, Rudd 1966, Eland and Danby 1968). Very recently it has been shown (Green and

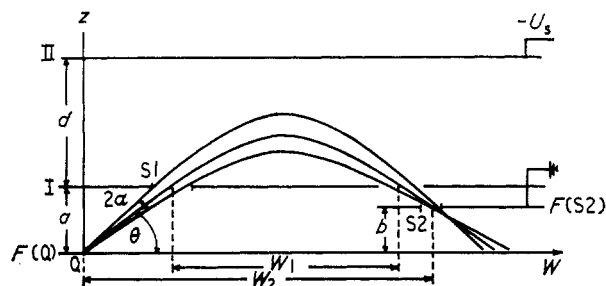


Figure 1 Electron trajectories in a parallel plate spectrometer of general type. Symbols are defined in the text

Proca 1970, Proca and Green 1970) that the addition of a field-free section to the normal parallel plate analyser will yield second order focusing. Because the second order focusing occurs for the entrance angle $\theta = \pi/6$ relative to the spectrometry plates (see figure 1), we will call this device a $\pi/6$ parallel-plate spectrometer. For the usual parallel-plate analyser with first order focusing we will use the name $\pi/4$ spectrometer. The first nonzero term of the $\pi/6$ spectrometer is of third order and negative. Therefore the minimum trace width of the electron beam occurs in a plane which lies in front of the plane containing the second order image. The analyser with the exit slit in the plane of minimum trace width will be called the modified $\pi/6$ spectrometer.

In the next section the optical properties of the three different parallel plate spectrometers using point sources will be investigated. In order to compare the properties of the parallel plate spectrometers with those of the cylindrical mirror and spherical analysers, we will consider first the case of rotational symmetry ($\Delta\phi = 2\pi$) of the parallel plate spectrometers (§3.1). Edelmann and Ulmer (1965) have suggested the name fountain spectrometer for this case of 2π geometry. Fountain spectrometers have the disadvantage of requiring large ring detectors, so in general a conventional detector will not be suitable. Using commercial electron detectors, only a small angular range $\Delta\phi \ll 2\pi$ of the fountain spectrometer contributes to the transmission. Resolution as a function of transmission will be evaluated for equal size detectors (§3.2) for the different parallel plate spectrometers which have the shape of a sector fountain spectrometer. We prefer this geometry because circular entrance and exit slits are better suited to a point source than rectangular slits.

2 Analysis of the parallel plate spectrometer

2.1 Focusing properties

In figure 1 the trajectories of electrons of energy $E = eU_e$ in the parallel-plate analyser of general type are shown. Electrons are emitted by a point source Q, located in a plane $F(Q)$ distance a from the lower capacitor plate I, and enter the uniform electric field through slit S1 at angles θ relative to the capacitor plate I. The exit slit S2 lies in a plane $F(S2)$ distance b ($0 \leq b \leq a$) from $F(Q)$. The projection W of the flight path between source and slit S2 on the plane $F(Q)$ is given by

$$W(\theta, K) = 2a\{(1 - B) \cotan \theta + K \sin 2\theta\} \quad (1)$$

where

$$K = \frac{d U_e}{a U_s} \quad (2a)$$

$$B = \frac{b}{2a} \quad (2b)$$

and U_s is the voltage applied between the two capacitor plates I and II.

† Now at Department of physics, University of Freiburg, Germany

The different types of parallel plate spectrometers can be derived from equation (1).

2.1.1 $\pi/4$ spectrometer Here the parameters B and a have the values $B=a=0$. With this, equation (1) becomes

$$W_1(\theta, U_e, U_s) = 2d \frac{U_e}{U_s} \sin 2\theta. \quad (3)$$

Because

$$\left(\frac{\partial W_1}{\partial \theta} \right)_{\theta_1 = \pi/4} = 0$$

and

$$\left(\frac{\partial^2 W_1}{\partial \theta^2} \right)_{\theta_1} = -8d \frac{U_e}{U_s} \neq 0$$

the $\pi/4$ spectrometer has first order focusing. The critical spectrometer voltage $U_s = U_{s,e}$, for which electrons of energy eU_e enter the spectrometer at $\theta_1 = \pi/4$ and leave the exit slit, is given by equation (3) to be

$$U_{s,e} \left(\frac{\pi}{4} \right) = \frac{2d}{W_{1,0}} U_e. \quad (4)$$

Here $W_{1,0}$ is the source-exit slit distance; both are located in the lower capacitor plate I.

2.1.2 $\pi/6$ spectrometer (i) With the choice of the parameters $B=0$, $a \neq 0$ equation (1) becomes

$$W_2(\theta, K) = 2a \{ \cotan \theta + K \sin 2\theta \}. \quad (5)$$

From

$$\frac{\partial W_2}{\partial \theta} = 0$$

it follows that

$$K = 1/(2 \sin^2 \theta \cos 2\theta),$$

and

$$\frac{\partial^2 W_2}{\partial \theta^2} = 0 \quad (6)$$

gives the equation

$$K = 1/4 \sin^4 \theta. \quad (7)$$

Equations (6) and (7) have the simultaneous solution $\theta_2 = \pi/6$, $K_2 = 4$.

Because

$$\left(\frac{\partial^3 W_2}{\partial \theta^3} \right)_{\theta_2, K_2} = -192a \neq 0,$$

the $\pi/6$ spectrometer has second order focusing. The critical spectrometer voltage $U_{s,e}$ is given by equation (2a) and $K=4$ to be

$$U_{s,e} \left(\frac{\pi}{6} \right) = \frac{d}{a} \frac{U_e}{K_2} = \frac{d}{4a} U_e. \quad (8)$$

(ii) For the more general case $0 < B \leq \frac{1}{2}$, $a \neq 0$, equation (1) becomes

$$W_2'(\theta, K') = 2a(1-B) \{ \cotan \theta + K' \sin 2\theta \} \quad (9)$$

where

$$K' = K/(1-B). \quad (10)$$

Equation (9) is the same as equation (5) except for the factor $(1-B)$. Therefore we expect second order focusing for $\theta_2 = \pi/6$ and $K'=4$, i.e., any parallel plate spectrometer with $0 \leq b \leq a$ possesses the property of second order focusing.

2.1.3 Modified $\pi/6$ spectrometer The first nonzero term of the Taylor series

$$\Delta W_2 = W_2(\theta_2 + \alpha, K_2) - W_2,0 = \sum_{n=1}^{\infty} \frac{1}{n!} \left(\frac{\partial^n W_2}{\partial \theta^n} \right)_{\theta_2, K_2} (\alpha)^n$$

is given by $-32a\alpha^3$, where α is the semi-angular aperture of the electron beam (see figure 1). Because of the odd order of

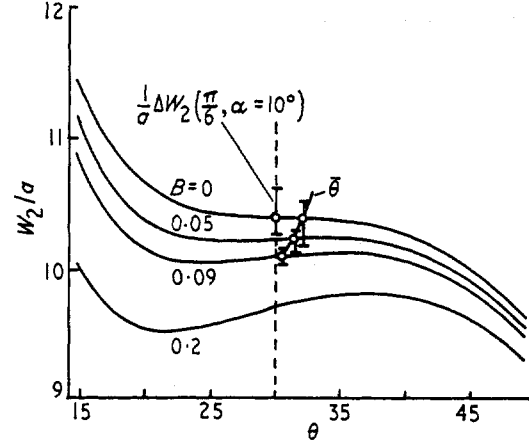


Figure 2 Reduced length W_2/a as a function of θ according to equation (11) with B as parameter. $B=0$ defines the plane with second order focusing. In planes with $B>0$ we have two local extrema of W_2/a but no second order focusing. For the aperture $2\alpha=20^\circ$, the minimum trace width occurs at the plane with $B=0.090$. This figure defines also the optimum mean entrance angle $\hat{\theta}$

the aberration term, there exists a plane different from the image plane where the trace width of the electron beam has a minimum. The negative sign of the aberration coefficient indicates that this plane lies above the plane $F(Q)$ (Hafner *et al.* 1968). In figure 2 reduced lengths W_2/a according to

$$W_2/a = 2\{(1-B) \cotan \theta + 4 \sin 2\theta\} \quad (11)$$

are plotted as functions of θ for different values of B .

For a full-angular aperture of $2\alpha=20^\circ$, for example, the electron beam has its minimum width at $B=0.090$. In figure 2 the optimal mean entrance angle $\hat{\theta}$ is also shown. Here $\hat{\theta}$ is defined by the requirement that

$$\Delta W_2 = W_2(\hat{\theta} - \alpha, B) - W_2(\hat{\theta} + \alpha, B)$$

where $W_2(\theta, B)$ is given by equation (11), becomes a minimum for a given α and B . $\hat{\theta}$ coincides with $\pi/6$ only for small values of α . For increasing aperture the deviation of $\hat{\theta}$ from $\pi/6$ increases. In the following, the properties of the $\pi/6$ spectrometer will be determined assuming $\hat{\theta} = \pi/6$, whereas for the modified spectrometer we will use the true optimal value of $\hat{\theta}$. For the $\pi/4$ spectrometer the optimal value of $\hat{\theta}$ is $\pi/4$, independent of α .

2.2 Base resolution

If $\Delta W(2\alpha)$ is the beam width at the exit slit corresponding to a full-angular aperture of 2α to a point source, and ΔS is the width of the exit slit, then the base resolution R^0 is given by

$$R^0 = \{\Delta W(2\alpha) + \Delta S\}/D \quad (12)$$

where

$$D = U_e \left(\frac{\partial W}{\partial U_e} \right)_{\theta, K} \quad (13)$$

defines the energy dispersion of the spectrometer. At optimum conditions the width $\Delta W(2\alpha)$ due to the aberration and the slit width ΔS contribute equally to the base resolution, and equation (12) becomes

$$R^0 = 2\Delta W(2\alpha)/D. \quad (14)$$

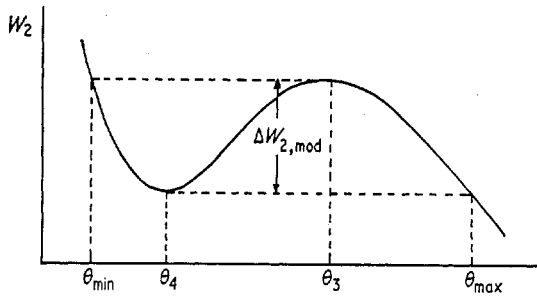


Figure 3 Shape of W_2 as function of θ in a plane with $B > 0$

The width $\Delta W(2\alpha)$ can be given as exact expressions for the different spectrometers:

$$\Delta W_{1,\pi/4}(2\alpha) = 4d \frac{U_e}{U_s} \sin^2 \alpha \quad (15a)$$

$$\Delta W_{2,\pi/6}(2\alpha) = 32a \frac{\sin 2\alpha \sin^2 \alpha}{1 - 4 \sin^2 \alpha} \quad (15b)$$

2.2.1 Modified $\pi/6$ spectrometer In figure 3 the shape of length W_2 as a function of θ , for $B > 0$, is shown. The optimal value of B for a given aperture 2α is $\theta_{\max} - \theta_{\min}$ if the trace width $\Delta W(2\alpha)$ becomes a minimum. From figure 3 it can be seen that this will be the case for the conditions $W_2(\theta_3) = W_2(\theta_{\min})$ and $W_2(\theta_4) = W_2(\theta_{\max})$. The values θ_3 , θ_4 , θ_{\min} and θ_{\max} can be derived from equation (11) and $\partial W_2 / \partial \theta = 0$ as

$$\sin \theta_{3/4} = \frac{1}{2}(1 \pm B^{1/2})^{1/2} \quad (16a)$$

and

$$\sin \theta_{\max/\min} = \frac{1}{2}(1 \pm B^{1/2}), \quad (16b)$$

where the upper and lower signs correspond to the subscripts 3, 4 and max, min respectively. With equation (16b) the optimum value of B and the optimum mean entrance angle

$$\bar{\theta} = \frac{1}{2}(\theta_{\min} + \theta_{\max})$$

can be evaluated for given apertures

$$2\alpha = \theta_{\max} - \theta_{\min}.$$

From equations (16b) and (11) the exact trace width $\Delta W_{2,\text{mod}}$ of the modified $\pi/6$ spectrometer is given by (see figure 3)

$$\begin{aligned} \Delta W_{2,\text{mod}}(2\alpha) &= W_{2,\text{mod}}(\theta_{\min}) - W_{2,\text{mod}}(\theta_{\max}) \\ &= 2a\{(3 - B^{1/2})^{3/2}(1 + B^{1/2})^{1/2} \\ &\quad - (3 + B^{1/2})^{3/2}(1 - B^{1/2})^{1/2}\}. \end{aligned} \quad (16c)$$

The energy dispersions are given by equations (3), (5) and (13):

$$D_{\pi/4} = 2dU_e/U_s \quad (17a)$$

$$D_{\pi/6} = 4\sqrt{3}a \quad (17b)$$

$$\begin{aligned} D_{\text{mod}} &= 8a \sin 2\bar{\theta} \\ &= 2a[(1 - B^{1/2})\{4 - (1 + B^{1/2})^2\}^{1/2} + (1 + B^{1/2}) \\ &\quad \times \{4 - (1 - B^{1/2})^2\}^{1/2}]. \end{aligned} \quad (17c)$$

The base resolutions are, from equations (15) and (17),

$$R^0_{\pi/4} = 4 \sin^2 \alpha \quad (18a)$$

$$R^0_{\pi/6} = \frac{16 \sin 2\alpha \sin^2 \alpha}{\sqrt{3} (1 - 4 \sin^2 \alpha)} \quad (18b)$$

$$\begin{aligned} R^0_{\text{mod}} &= \\ &= \frac{2(3 - B^{1/2})^{3/2}(1 + B^{1/2})^{1/2} - (3 + B^{1/2})^{3/2}(1 - B^{1/2})^{1/2}}{(1 - B^{1/2})\{4 - (1 + B^{1/2})^2\}^{1/2} + (1 + B^{1/2})\{4 - (1 - B^{1/2})^2\}^{1/2}}. \end{aligned} \quad (18c)$$

2.3 Transmission

The transmission for a point source at optimum conditions $\{\Delta W(2\alpha) = \Delta S\}$ and with the choice of the angle θ (see figure 1) is given by

$$T = \frac{\Delta\phi}{4\pi} (\sin \theta_{\max} - \sin \theta_{\min}) \quad (19a)$$

$$= \frac{\Delta\phi}{2\pi} \cos \bar{\theta} \sin \alpha. \quad (19b)$$

For $\Delta\phi = 2\pi$ we have

$$T_{\pi/4} = \frac{\sqrt{2}}{2} \sin \alpha \quad (20a)$$

$$T_{\pi/6} = \frac{\sqrt{3}}{2} \sin \alpha \quad (20b)$$

$$T_{\text{mod}} = \frac{1}{2} B^{1/2}. \quad (20c)$$

Equation (20c) follows from equations (19a) and (16b).

3 Comparison of spectrometers

3.1 2π geometry

Edelmann and Ulmer (1965) have introduced the $\pi/4$ parallel plate spectrometer with $\Delta\phi = 2\pi$ (fountain spectrometer). Figure 4 represents schematically a modified $\pi/6$ fountain spectrometer. In spite of the 2π integration it has the disadvantage of the large ring detector, which prevents single particle detection in general.

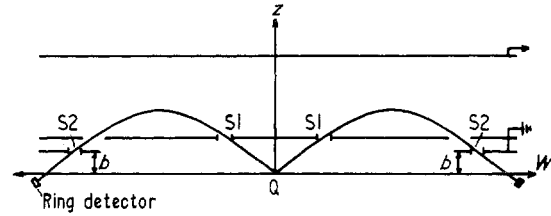


Figure 4 Schematic representation of a modified $\pi/6$ -fountain spectrometer

For fountain spectrometers the base resolution R^0 as function of transmission T is given by equations (18) and (20)

$$R^0_{\pi/4} = 8T^2 \quad (21a)$$

$$R^0_{\pi/6} = \frac{256 T^3 (1 - 4T^2/3)^{1/2}}{9 (1 - 16T^2/3)} \quad (21b)$$

$$\begin{aligned} R^0_{\text{mod}} &= \\ &= \frac{2(3 - 2T)^{3/2}(1 + 2T)^{1/2} - (3 + 2T)^{3/2}(1 - 2T)^{1/2}}{(1 - 2T)\{4 - (1 + 2T)^2\}^{1/2} + (1 + 2T)\{4 - (1 - 2T)^2\}^{1/2}} \quad (21c) \\ &= 4T^3/(1 + \frac{4}{3}T^2) \quad \text{for } T \ll 1. \end{aligned} \quad (21d)$$

Figure 5 shows the base resolutions R^0 as function of the transmission T for the three fountain spectrometers. The mean entrance angle $\bar{\theta}$ and the reduced distance B of the modified spectrometer are also plotted. From figure 5 it follows that the $\pi/6$ fountain spectrometer is superior to the $\pi/4$ fountain spectrometer, the modified spectrometer is even better.

The base resolutions $R^0(T)$ of figure 5 have been evaluated using equations (21a-c), which are exact expressions except for the contribution from the energy dispersion, which becomes exact only as $T \rightarrow 0$. Thus we expect for large T ($T > 10\%$) deviations between the exact base resolution and the approximations of equations (21a-c). Table 1 compares

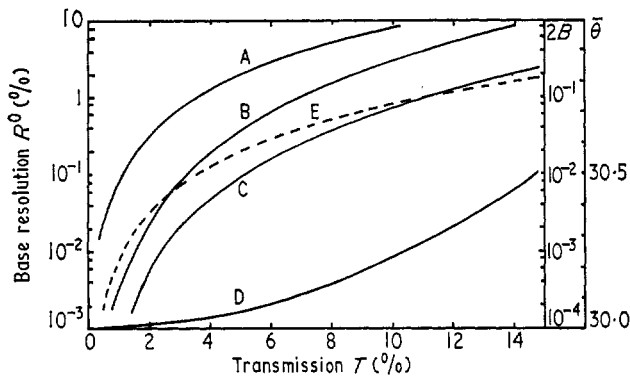


Figure 5 Base resolutions R^0 of parallel plate spectrometers with 2π geometry: A, $\pi/4$ spectrometer; B, $\pi/6$ spectrometer; C, modified $\pi/6$ spectrometer; D, mean entrance angle $\bar{\theta}$ of modified $\pi/6$ spectrometer; E, reduced distance B of plane with minimum trace width

for this reason the exact and approximate base resolutions for $T=15\%$.

In figure 6 we compare the base resolutions of our proposed parallel plate analysers with 2π geometry with other electrostatic analysers also having a 2π geometry (cylindrical mirror analyser and spherical plate analyser). The base resolutions of the latter analysers have been taken from Hafner *et al.* (1968). Figure 6 indicates that the modified $\pi/6$ fountain spectrometer is superior even to the cylindrical mirror analyser.

Table 1 Base resolutions of fountain spectrometers in % for transmission $T=15\%$

Spectrometer	Exact (%)	Equations (21a-c) (%)
$\pi/4$	18.9	18.0
$\pi/6$	12.3	10.7
modified	3.06	2.45

3.2 $\Delta\phi \ll 2\pi$

A serious drawback of the fountain spectrometers is the difficulty of single particle detection. Because circular slits are better suited to a point source than rectangular slits, we investigated the properties of parallel plate analysers with sector shape ($\Delta\phi \ll 2\pi$). A particle detector with fixed length l_D defines an angular region $\Delta\phi$, which is different for the three types of analysers. Figure 7 shows the projection of a sectional parallel plate analyser. For comparison of the different analysers we require that the analysers have about equal dimensions. This will be the case assuming (i) the distance d of the capacitor plates is the same for all three types, and (ii) electrons of energy eU_e are detected in all cases by applying the same critical voltage $U_{s,e}$ between the capacitor plates.

Assumption (ii) together with equations (4) and (8) yields the source-exit slit distance of the $\pi/4$ spectrometer to be $W_{1,0} = 8a$. For comparison the corresponding distances of the $\pi/6$ and modified spectrometer are $W_{2,0} = \sqrt{3}(6-2B)a$.

The length $l_D = a$ of the detector, and transmission T of the spectrometer determine an angular region $\Delta\phi$ and from equation (19b) an aperture 2α . Both are plotted in figure 8

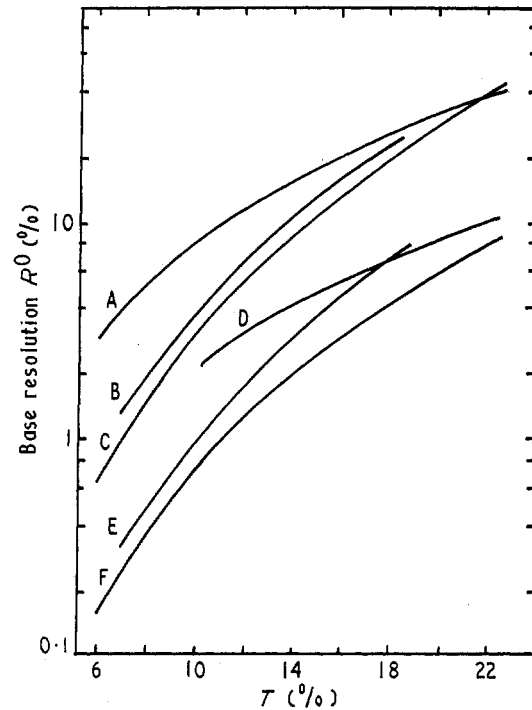


Figure 6 Base resolution R^0 of electrostatic spectrometers with 2π geometry as function of transmission T . A, $\pi/4$ parallel plate; B, cylindrical mirror, exit slit at plane of second order focus; C, $\pi/6$ parallel plate, exit slit at plane of second order focus; D, 180° spherical plate; E, cylindrical mirror, exit slit at plane of minimum trace width; F, modified $\pi/6$ parallel plate, exit slit at plane of minimum trace width. The curves B, D and E are reproduced from figure 4 of Hafner *et al.* (1968)

as functions of the transmission for the three parallel plate spectrometers. The mean entrance angle $\bar{\theta}$ of the modified spectrometer is also given. The apertures 2α of figure 8 have been used to calculate the base resolutions R^0 with equations (18a-c). These are given as functions of the transmission T in figure 9 together with the distance B of the modified spectrometer. This figure indicates that only for $T < 0.215\%$ is the sector shaped $\pi/6$ spectrometer superior to the $\pi/4$ spectrometer. In any case, the modified spectrometer here also has the best optical properties.

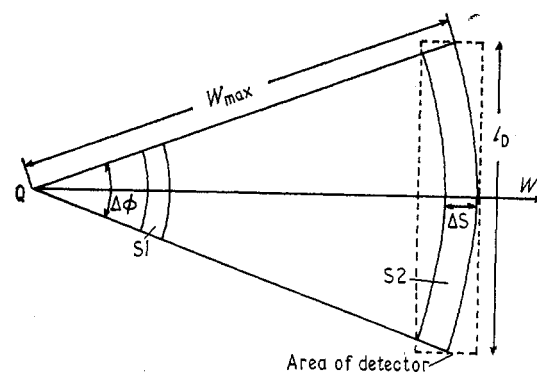


Figure 7 Projection of sector shaped parallel plate spectrometer on plane $F(Q)$

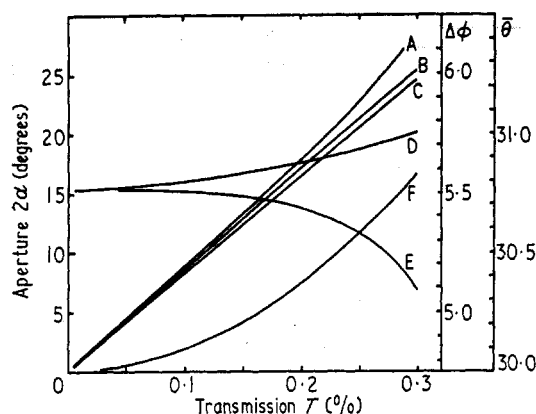


Figure 8 Full-angular aperture 2α and angular regions $\Delta\phi$ of sector shaped parallel plate spectrometers as functions of transmission T : A, 2α of $\pi/6$ spectrometer; B, 2α of modified $\pi/6$ spectrometer; C, 2α of $\pi/4$ spectrometer; D, $\Delta\phi$ of modified $\pi/6$ spectrometer; E, $\Delta\phi$ of $\pi/6$ spectrometer; F, mean entrance angle θ of modified $\pi/6$ spectrometer. $\Delta\phi$ of the $\pi/4$ spectrometer is 7.17° , independent of transmission T

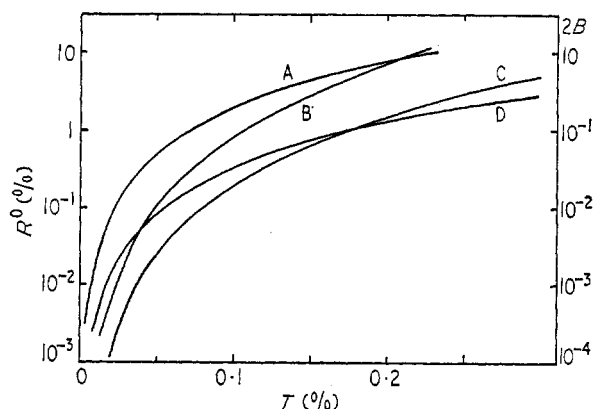


Figure 9 Base resolution R^0 of sector shaped parallel plate spectrometers as a function of transmission T . A, $\pi/4$ spectrometer; B, $\pi/6$ spectrometer; C, modified $\pi/6$ spectrometer; D, reduced distance B of plane with minimum trace width

4 Conclusions

In this paper it has been shown that the parallel plate analyser in the modified $\pi/6$ form is superior to the $\pi/4$ form, which has been used so far. For equal transmission the base resolution can be improved by a factor of 5 to 10. In the 2π geometry the modified $\pi/6$ parallel plate analyser for point sources is superior to all other electrostatic analysers, although there remains the problem of large ring shaped particle detectors.

Acknowledgments

We are grateful to Dr K D Sevier for reading the manuscript and improving the style.

References

- Aksela S, Karras M, Pessa M and Suoninen E 1970 *Rev. Sci. Instrum.* **41** 351-5
- Blauth E 1957 *Z. Phys.* **147** 228-40
- Edelmann F and Ulmer K 1965 *Z. Angew. Phys.* **18** 308-15
- Eland J D H and Danby C J 1968 *J. Phys. E: Sci. Instrum.* **1** 406-8

Green T S and Proca G A 1970 *Rev. Sci. Instrum.* **41** 1409-14

Gremmelmaier R 1952 *PhD Thesis* Technische Hochschule Karlsruhe

Hafner H, Simpson J A and Kuyatt C E 1968 *Rev. Sci. Instrum.* **39** 33-5

Harrower G H 1955 *Rev. Sci. Instrum.* **26** 850-4

Hughes A L and Rojansky 1929 *Phys. Rev.* **34** 284-90

Lassettre E N, Berman A S, Silverman S M and Krasnow M E 1964 *J. Chem. Phys.* **40** 1232-42

Mehlhorn W 1960 *Z. Phys.* **160** 247-67

Proca G A and Green T S 1970 *Rev. Sci. Instrum.* **41** 1778-83

Purcell E M 1938 *Phys. Rev.* **54** 818-26

Rudd M E 1966 *Rev. Sci. Instrum.* **37** 971-3

Sar-El H Z 1967 *Rev. Sci. Instrum.* **38** 1210-6

Zashkvara V V, Korsunskii M I and Kosmachev O S 1966 *Soviet Phys.-tech. Phys. (English transl.)* **11** 96-102